MASTER EM3E-4SW

Academic year 2018-2019

Erasmus Mundus Master in Membrane Engineering for a Sustainable World

Semester 4

Master Thesis Project

Development of Ceramic-Supported 2D Nanosheet Membranes for Organic Solvent Nanofiltration

(Annex)

VILLICAÑA GONZÁLEZ Eduardo

28.06.2019

Supervisor: Marie-Alix Pizzoccaro-Zilamy, m.d.pizzoccaro@utwente.nl; Mieke Luiten-Olieman , m.w.j.luiten@utwente.nl.

Overseer: Reyes Mallada, r.mallada@unizar.es.

Annex Index

Annex 1. *Synthesis of 2D $Ni(OH)_2$ nanosheets by co-precipitation for preparation of membranes.*

At one first approach, 2D $Ni(OH)_2$ nanosheet based membranes were prepared based on the work performed by Qu and co-workers [1]. This procedure is based on the chemical precipitation method which consists in the formation of $Ni(OH)_2$ nanosheets by the quick addition of an ethanolamine solution to a nickel (II) nitrate solution (dispersion noted NHN-1 in exp. part). When the pH is sufficiently high, the hydroxide anion concentration exceeds the solubility limit of the $Ni(OH)_2$ produce which thus a precipitate [2]. Following the same procedure, a first membrane was prepared on top of a PES support (200 nm in pore size). Figure A. 1B shows the cross-section SEM image of the membrane denoted NiNM/PES. The SEM pictures allow us to clearly observe the ~700 nm thick $Ni(OH)_2$ nanosheets layer on top of the PES support. Compare to the surface of the pristine support (Figure A. 1A), the deposited layer of $Ni(OH)_2$ nanosheets shows a quite smooth surface.

Nevertheless, this method presented a problem of reproducibility in terms of particle size. The particle size distribution of the resulting mixture from the co-precipitation reaction was obtained by dynamic light scattering (DLS). Although DLS analysis is not exact since the equipment measures the particle size assuming a spherical shape of the particles, it gives a good approximation of the particles size. As an example, when the suspension analyzed in Figure A. 3B was filtered through a PES support (200 nm in pore size), nothing was retained, and thus, no membrane was obtained with this sample. However, using this same solution it was possible to obtain a film when the dispersion was filtered through a cellulose nitrate support with 25 nm in pore size.

Hall and co-workers [2], highlighted that the base addition speed during a nucleation process is typically dropwise. Such conditions are not specified in the procedures described in the literature [1,3]. In order to understand the problem of reproducibility of the Nickel Hydroxide nanosheets membranes, two different Nickel Hydroxide nanosheets (NHD) dispersions were prepared using either a quick addition (NHD-QA) or a dropwise addition (NHD-DW) of the ethanolamine solution to the Nickel (II) nitrate solution. However, the improvement in the reproducibility of the final particle size was not achieved.

The membranes obtained on cellulose nitrate support ($Ø_{pore} \approx 25$ nm), denote NiNM/CN, were tested to assess the retention properties PEG and methylene blue. Figure

A. 2 shows the Methylene Blue (MB) retention results of the NiNM/CN samples. The NiNM/CN-1 membrane present a higher MB rejection than the NiNM/CN-2 membrane (62% instead of 18%). These results can be explained by the difference of nanosheets size between the two membranes. For PEG, no rejection was achieved.

Using the procedure described by Qu and workers [1], it is impossible to prepare identical 2D $Ni(OH)_2$ nanosheets membranes. These irreproducible results are due to the impossibility to control the spontaneous nucleation during co-precipitation at room temperature [4].

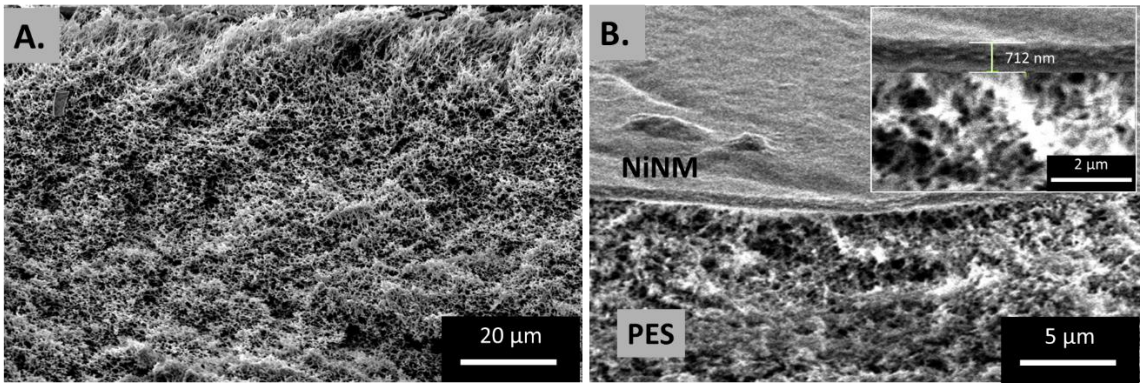

Figure A. 1. Cross-sectional SEM pictures of the pristine PES support (A.) and the NiNM/PES membrane (B.).

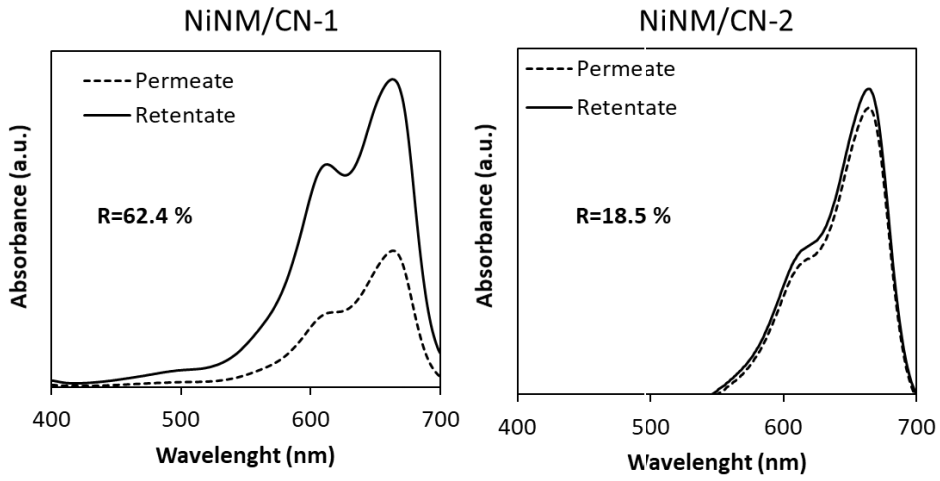

Figure A. 2. Methylene blue spectra from the samples of the MB retention analysis.

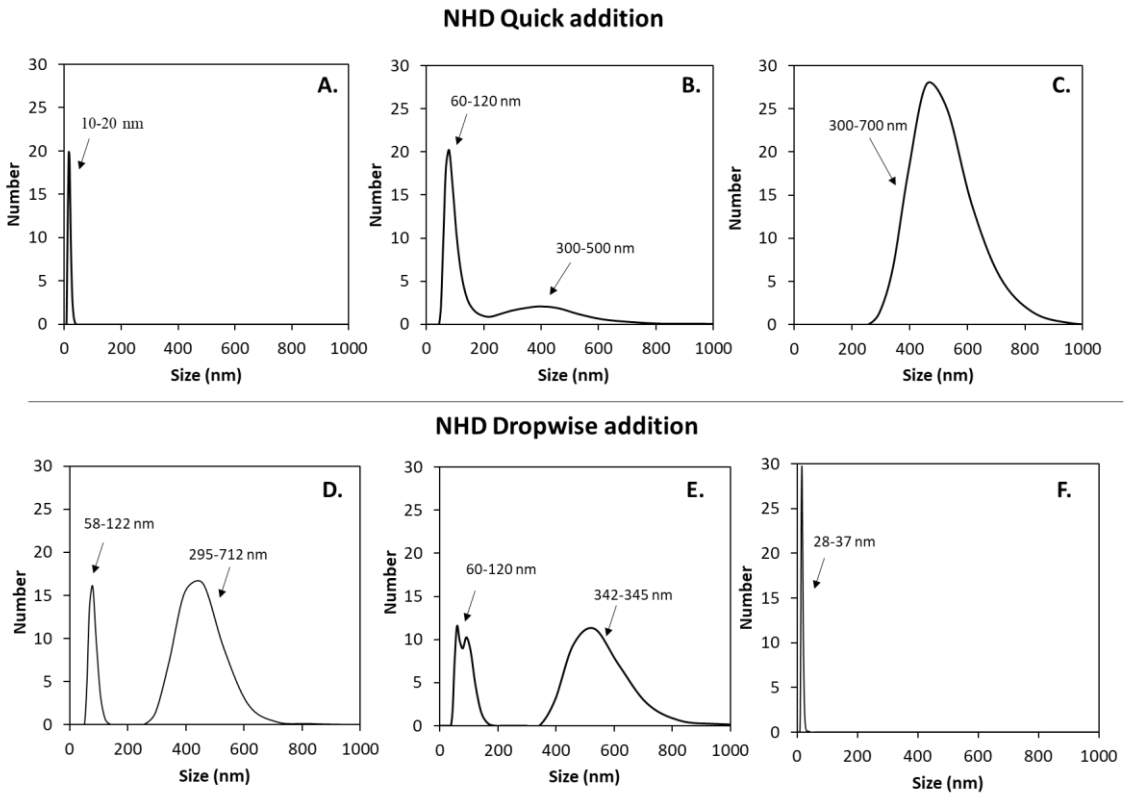

Figure A. 3. Particle size distribution obtained by DLS for 3 different dispersions: prepared by quick addition (A., B., C.) and by dropwise addition (D., E., F.) of the ethanolamine solution.

[1] Y. Qu, Q.G. Zhang, F. Soyekwo, R.S. Gao, R.X. Lv, C.X. Lin, M.M. Chen, A.M. Zhu, Q.L. Liu, Nickel hydroxide nanosheet membranes with fast water and organics transport for molecular separation, Nanoscale. 8 (2016) 18428–18435. doi:10.1039/C6NR06612G.

[2] Hall David S., Lockwood David J., Bock Christina, MacDougall Barry R., Nickel hydroxides and related materials: a review of their structures, synthesis and properties, Proceedings of the Royal Society A: Mathematical, Physical and Engineering Sciences. 471 (2015) 20140792. doi:10.1098/rspa.2014.0792.

[3] H. Ang, L. Hong, Engineering defects into nickel-based nanosheets for enhanced water permeability, J. Mater. Chem. A. 5 (2017) 20598–20602. doi:10.1039/C7TA06908A.

[4] J.W. Mullin, Crystallization, Elsevier, 2001.

Annex 2. *Schematic representation of the different synthesis methods employed during this project.*

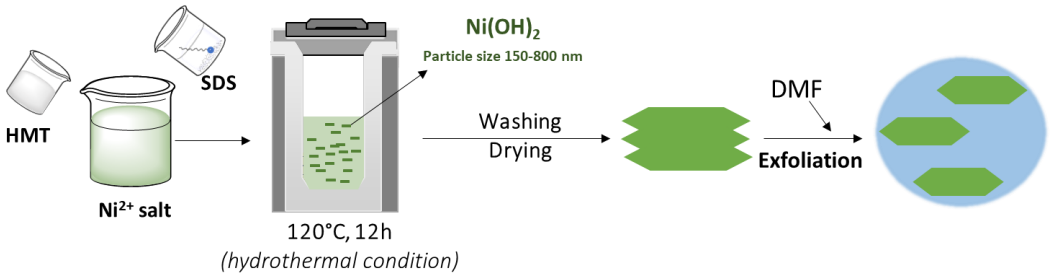

Figure A. 4. $Ni(OH)_2$ nanosheet synthesis by hydrothermal treatment and exfoliation.

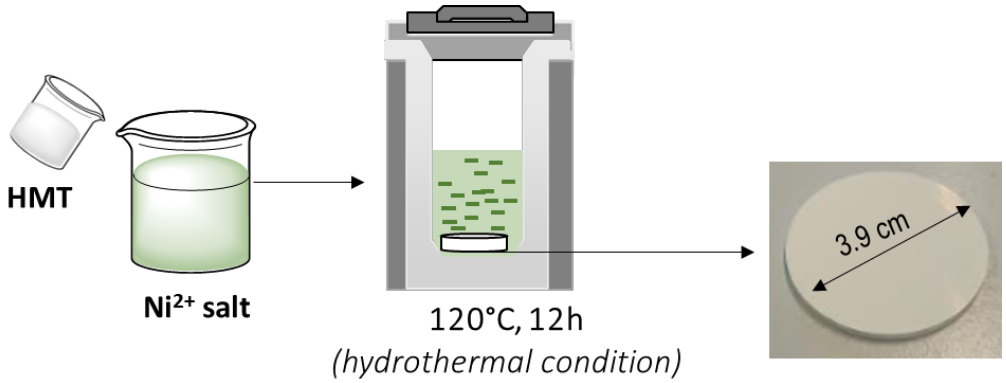

Figure A. 5. Schematic illustration of $Ni(OH)_2$ based membrane by in situ growth.

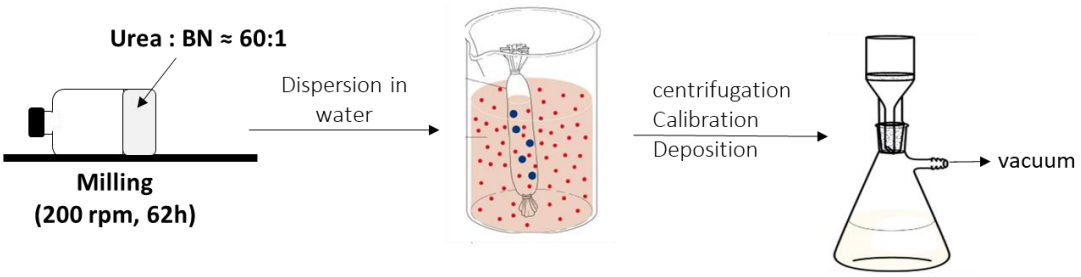

Figure A. 6. Schematic illustration of functionalized *h*-BN membranes preparation.

Annex 3. *Additional information about 2D $Ni(OH)_2$ nanosheet dispersion*

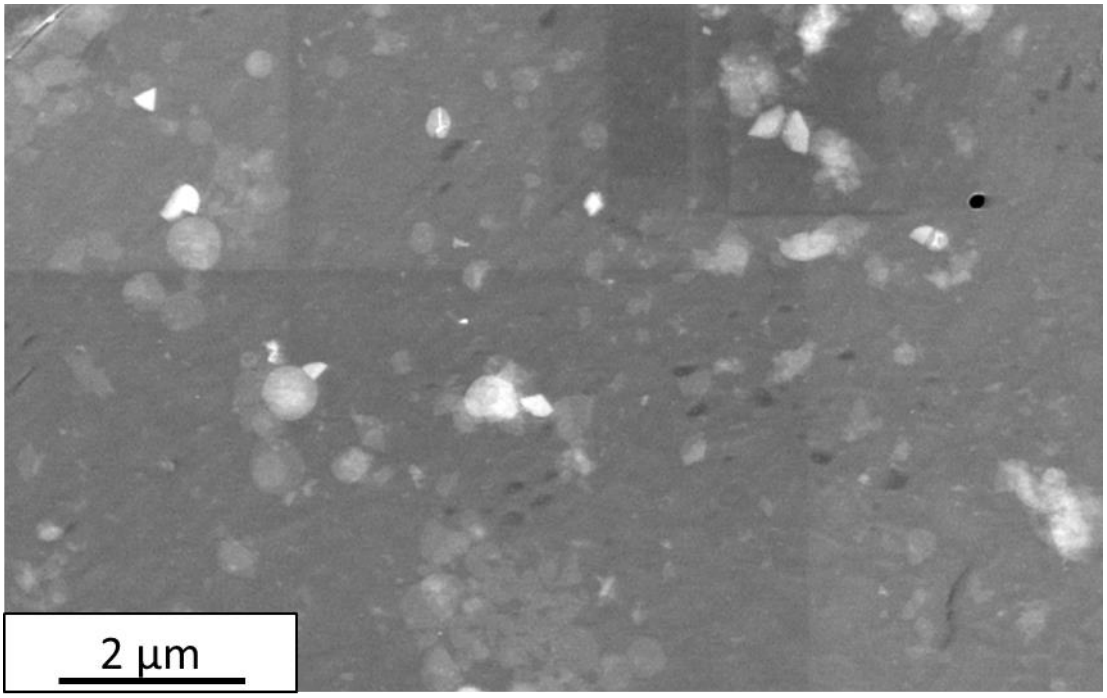

Figure A. 7. STEM-in-SEM image employed for particle size distribution analysis in software Image J.

Annex 4. *Additional results for 2D layered $Ni(OH)_2$ crystals based membrane.*

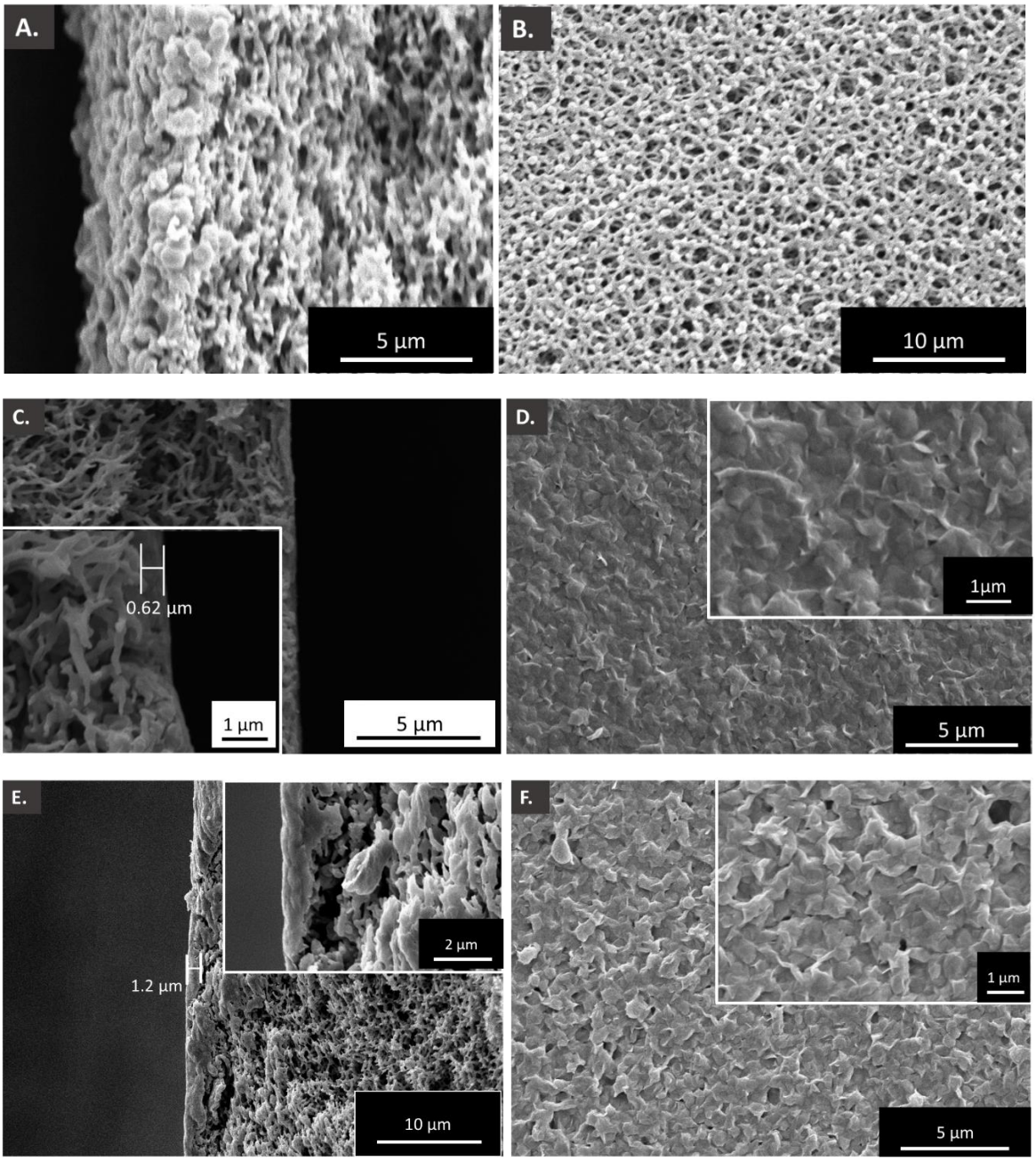

Figure A. 8. SEM images of NiLM. (A. and B.) Cross section and surface of NiLM-1. The image suggest that no layer was formed on the surface. However, the results show a considerable decrease of the permeability compared to PES support. Therefore, layered $Ni(OH)_2$ could be trapped in the inner structure of the support. (C. and D.) Cross section and surface of NiNL-2. (E- and F.) Cross section and surface of NiNL-3.

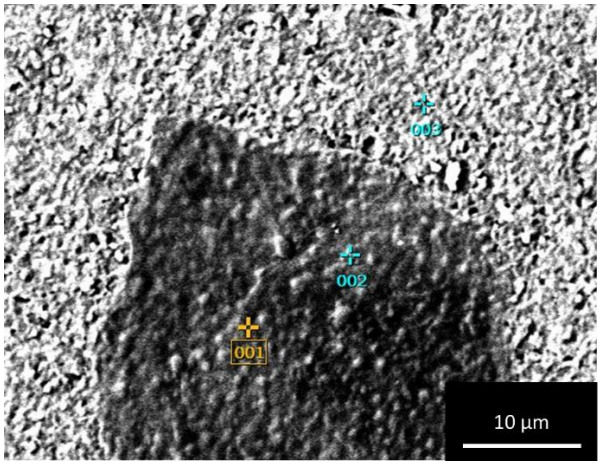

Point n°	Atom% Ni	Atom% S	Ni/S
1	4.66	5.35	0.87
2	4.14	5.64	0.73
3	7.54	5.72	1.31

Figure A. 9. EDX-in-SEM analysis of NiLMs to determinate composition of the layered composite forming the membrane. On this way, it was possible to estimate the final concentration of surfactant intercalated in the layered $Ni(OH)_2$ crystal.

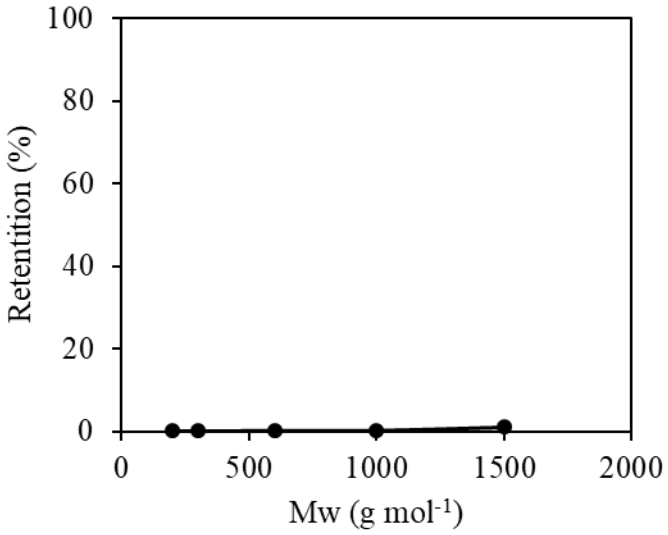

Figure A. 10. PEG-MWCO of NiLMs.

Figure A. 11. Image of NiNL-5. The formation of bubbles due the presence in excess of the surfactant led to multiple defects formation on the ceramic support.

Annex 5. *Additional results of $Ni(OH)_2$ membranes obtained by in situ growth*

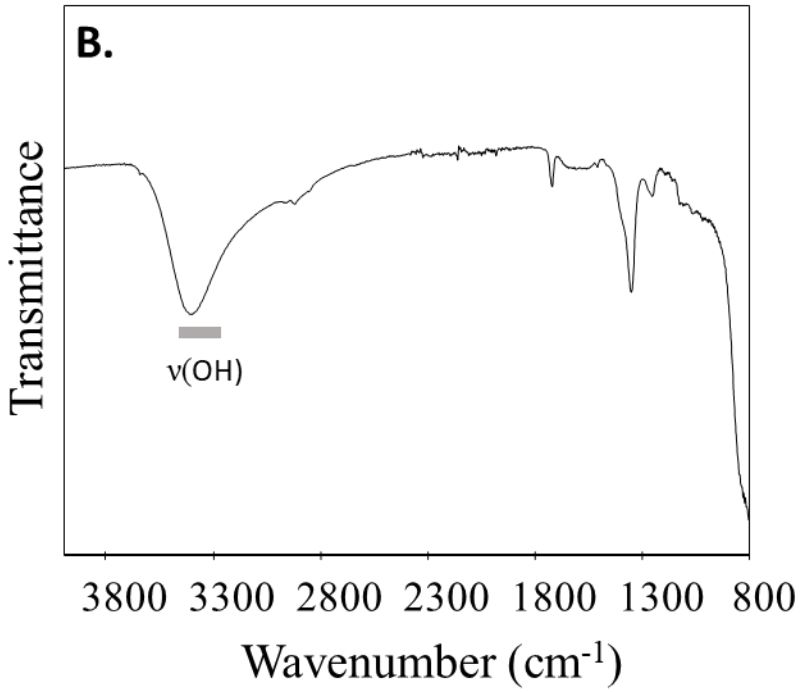

Figure A. 12. FTIR spectra of the resulting membrane from in situ growth to confirm the composition.

Annex 6. *MWCO measurements*

Gel permeation chromatography (GPC) analysed the composition of the feed, permeate, and retentate. The GPC setup consisted of two PSS SUPREMA columns: 1000 Å, 10 µm, 8 x 300 mm and 30 Å, 10 µm, 8 x 300 mm columns from PSS Polymer Standards Service GmbH (Germany), a HPLC pump from Agilent 1200 series modules. The columns were calibrated using 16 different PEG standards (Mw: 62 – 42 000 g mol^{-1}, PSS Polymer Standards Service GmbH, Germany). The GPC eluent consisted of pure water (MQ) containing 50 mg/mL NaN_3. For each GPC analysis, 100 µL of the sample were injected into the equipment, which ran at 1 mL min^{-1}. The rejection R was determined with Equation A1, where C_R and C_P are the concentrations of the dye in the retentate and the permeate respectively. To correct the inevitable accumulation of retained PEG molecules in a dead-end set up, the average of the original feed concentration and the final retentate concentration is used as C_R.

$$R = \left(1 - \frac{C_P}{C_R}\right) * 100 \quad \textbf{(A1)}$$

Puhlfurß et al. [38] correlated the molecular weight of PEG to Stokes-Einstein radius of molecules (Equation A.1). Besides, with this test is possible to characterize the MWCO of our membrane, obtaining thus information about its retention performance [33].

$$Molecular\ radius\ (\text{Å}) = 0.262 \times (Mw)^{\frac{1}{2}} - 0.3 \quad \textbf{(A.1)}$$

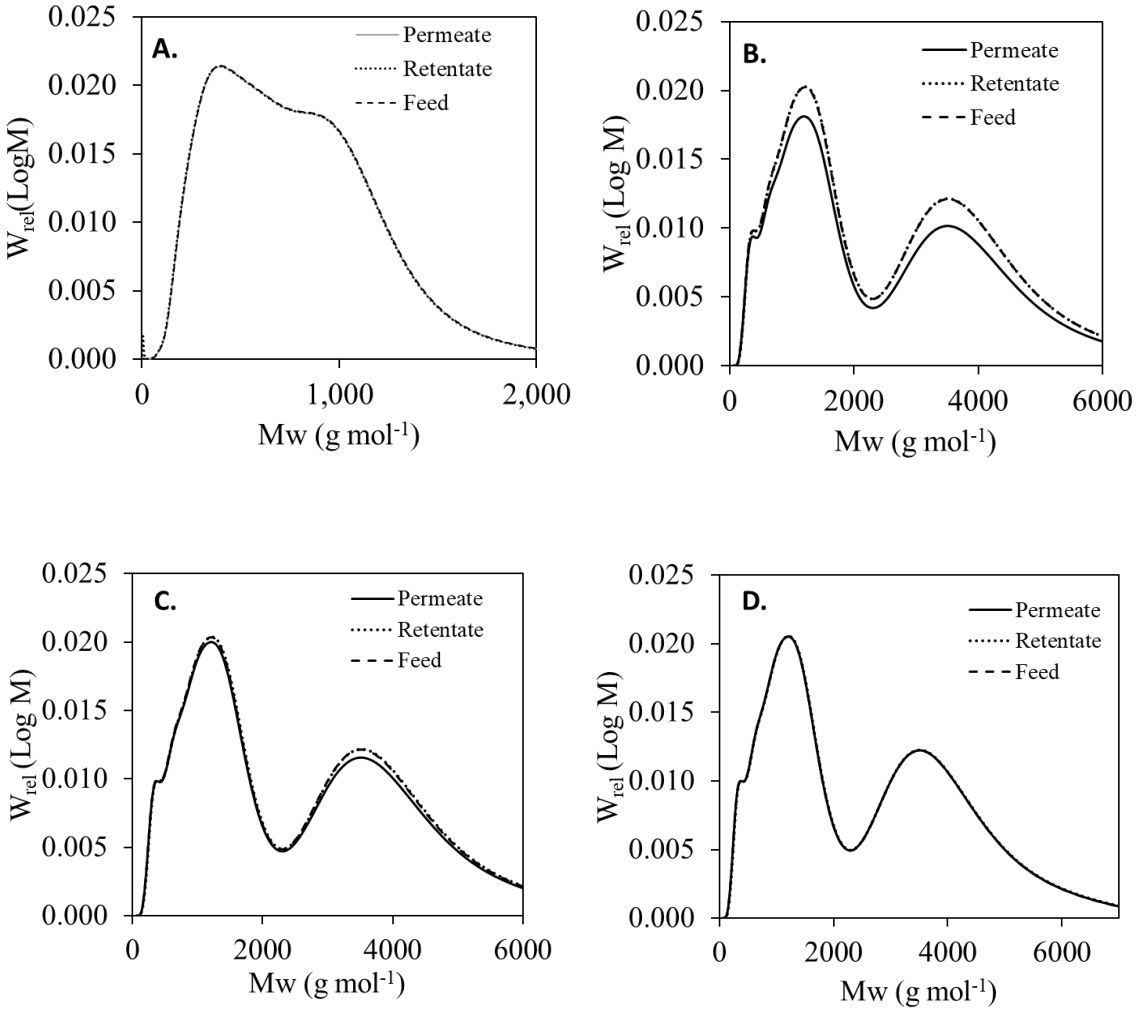

Figure A. 13. Molecular weight distribution of permeate, retentate, and feed for the membranes: (A.) NiLM. (B.) NiEx. (C.) $Ni(OH)_2$ by in situ growth. (D.) FBNM

Annex 7. *Comparison of the performance of different NF membranes*

Table A. 1. Comparison of the performance of different 2D inorganic nanosheet membranes with graphene, graphene oxide, and polyether sulfone.

Author	2D-NSM	Thickness (nm)	Support/ pore size	Permeance (L m^{-2} h^{-1} bar^{-1})	Rejection	No. R
Han et al.	Chemically covered graphene	25-53	-	21.4	99 % to most organic dyes	[1]
Ying et al.	Reoxidated pristine GO sheets	-	-	191	88.5% EB	[2]
Wang et al.	GO sheets with incorporated carbon nanodots	-	-	939	96% Rhodamine	[3]
Sun et al.	MoS_2 exfoliated nanosheets	1, 700	Polycarbonate 200 nm	245	89% EB	[4]
Sun et al.	WS_2 exfoliated nanosheets	500	Non-specified	930	89% EB	[5]
Qu et al.	Ni $(OH)_2$ nanosheets	3, 180	Alumina 200 nm	99	94% MB 89.6% MO 97% DY	[6]
Ang et al.	Ni $(OH)_2$ defect-rich nanosheets	641	Nylon	1330	96.4% MR 98.1% MO 98.2% EB	[7]
Chen et al.	BN exfoliated nanosheets	0.4	Nylon	1100	99% MB	[8]
Gao et al.	Reduced GO intercalated with TMPyP	34	Nylon	12.82	97% EB	[9]
Huang et al.	Solvated reduced GO	3.4	Nylon	87.6	100% EB	[10]
Huang et al.	Solvated reduced GO functionalized with HPEI	3.4	-	85.2	100% EB	[10]
Ang et al.	NF-PES-010	-	-	40	98% VB	[7]

[1] Y. Han, Z. Xu, C. Gao, Ultrathin Graphene Nanofiltration Membrane for Water Purification, Advanced Functional Materials. 23 (2013) 3693–3700. doi:10.1002/adfm.201202601.

[2] Y. Ying, L. Sun, Q. Wang, Z. Fan, X. Peng, In-plane mesoporous graphene oxide nanosheet assembled membranes for molecular separation, RSC Adv. 4 (2014) 21425–21428. doi:10.1039/C4RA01495B.

[3] W. Wang, E. Eftekhari, G. Zhu, X. Zhang, Z. Yan, Q. Li, Graphene oxide membranes with tunable permeability due to embedded carbon dots, Chem. Commun. 50 (2014) 13089–13092. doi:10.1039/C4CC05295A.

[4] L. Sun, H. Huang, X. Peng, Laminar MoS2 membranes for molecule separation, Chem. Commun. 49 (2013) 10718–10720. doi:10.1039/C3CC46136J.

[5] L. Sun, Y. Ying, H. Huang, Z. Song, Y. Mao, Z. Xu, X. Peng, Ultrafast Molecule Separation through Layered WS2 Nanosheet Membranes, ACS Nano. 8 (2014) 6304–6311. doi:10.1021/nn501786m.

[6] Y. Qu, Q.G. Zhang, F. Soyekwo, R.S. Gao, R.X. Lv, C.X. Lin, M.M. Chen, A.M. Zhu, Q.L. Liu, Nickel hydroxide nanosheet membranes with fast water and organics transport for molecular separation, Nanoscale. 8 (2016) 18428–18435. doi:10.1039/C6NR06612G.

[7] H. Ang, L. Hong, Engineering defects into nickel-based nanosheets for enhanced water permeability, J. Mater. Chem. A. 5 (2017) 20598–20602. doi:10.1039/C7TA06908A.

[8] C. Chen, J. Wang, D. Liu, C. Yang, Y. Liu, R.S. Ruoff, W. Lei, Functionalized boron nitride membranes with ultrafast solvent transport performance for molecular separation, Nature Communications. 9 (2018) 1902. doi:10.1038/s41467-018-04294-6.

[9] T. Gao, L. Huang, C. Li, G. Xu, G. Shi, Graphene membranes with tuneable nanochannels by intercalating self-assembled porphyrin molecules for organic solvent nanofiltration, Carbon. 124 (2017) 263–270. doi:10.1016/j.carbon.2017.08.042.

[10] L. Huang, J. Chen, T. Gao, M. Zhang, Y. Li, L. Dai, L. Qu, G. Shi, Reduced Graphene Oxide Membranes for Ultrafast Organic Solvent Nanofiltration, Advanced Materials. 28 (2016) 8669–8674. doi:10.1002/adma.201601606.